Jpn. J. Appl. Phys. Vol. 37 (1998) pp. 217–223
Part 1, No. 1, January 1998


# Reflective Supertwisted Nematic Liquid Crystal Displays

Jun CHEN, Fei-Hong YU*[1], Ho-Chi HUANG and Hoi S. KWOK*[2]
*Centre for Display Research and Department of Electrical and Electronic Engineering, Hong Kong University of Science and Technology, Clear Water Bay, Hong Kong*

(Received July 22, 1997; accepted for publication October 7, 1997)

Supertwisted nematic (STN) liquid crystal displays are widely used commercially. However, there is still room for improvement. In this paper, we discuss reflective STN displays in which the rear polarizer has been removed and no retardation film is used for dispersion compensation. This new design can potentially yield higher brightness than conventional STN displays. They can also have better chromaticity. Numerical calculations and experimental data on such reflective STN liquid crystal displays with twist angles of 190–240° are presented in this paper. These new displays have reasonably steep reflectance-voltage characteristics and can be multiplex-driven like ordinary transflective STN displays. An additional advantage of this new display is the absence of a viewing parallax if the reflector is placed inside the liquid crystal cell.

KEYWORDS: supertwisted nematic LCD, reflective LCD, parameter space

## 1. Introduction

Supertwisted nematic (STN)[1–3] liquid crystal displays (LCD) are used in many applications requiring high information content. Because of their steep electrooptic response curves, STN can be multiplex-driven.[4] Such passive matrix displays with 480 lines or more have been produced commercially and used in, for example, portable computers and personal data systems. With various film enhancement techniques and multiline driving schemes, the quality of STN displays is approaching that of active-matrix LCDs. In many cases, the STN operates in a transmittive mode with backlighting. Transflective displays where a reflector is placed at the back is also used, but their brightness is far from ideal. Quite often, retardation films are needed to correct the chromatic dispersion present in such STN displays. There clearly is still much room for improvement for these STN displays.

True reflective displays requiring no backlighting are desirable for low power and portable applications. Much effort has been devoted recently to improving the brightness and chromaticity of such reflective STN displays.[5] Considerable success has been achieved with reflective displays that do not require any polarizer, such as the bistable Cholesteric display,[6] and the guest-host display.[5] In this paper, we report a reflective display that is still based on the twisted nematic (TN) effect and polarization manipulation. However, unlike ordinary STN, this reflective STN (RSTN) display requires only one polarizer.[7–9] It consists simply of an input polarizer, an LC cell and a rear reflector which can be placed either inside or outside the LC cell. The elimination of the rear polarizer results in higher light efficiency due to less absorption and scattering losses. Moreover, we show that such RSTNs have a much better chromaticity than conventional STN. No dispersion compensation is needed to achieve a high contrast black/white display.

This RSTN is similar to the reflective nematic displays we discussed in two previous publications.[8,9] However, the display in ref. 8 requires a retardation film for dispersion compensation, while that in ref. 9 has a low twist and is not suitable for multiplexing. The RSTN discussed herein is designed specifically for passive-matrix low-power applications. The elimination of the rear polarizer also means that, potentially, the reflector can be placed inside the liquid crystal cell. Thus, the viewing parallax can be eliminated.

The RSTN is obtained through a systematic examination of the parameter space[7] of $\phi$, $\alpha$ and $d\Delta n$ for nematic LCDs, where $\phi$ is the twist angle, $\alpha$ is the polarizer angle, $d$ is the LC cell thickness and $\Delta n$ is the LC birefringence. We have achieved RSTNs with twist angles of 190–240°, similarly to ordinary STN. In the following sections, we first introduce the parameter space for reflective LCDs and discuss some general principles on how these parameter space diagrams can be used in the search for better display modes. Then, the numerical results for the RSTN using full dynamical simulation of the LCD will be discussed. Finally, experimental results of the RSTN using the optimized design parameters will be presented. It will be shown that there is a good agreement between the theoretical calculations and the experimental results. In general, the RSTN is capable of high brightness, low color dispersion and good contrast.

## 2. Parameter Space for the RSTN

The display geometry discussed here is the simplest possible for polarization manipulation; there is a front polarizer, an LC cell and a rear mirror. No retardation film will be employed in this study. For practical applications, a light diffuser should be part of the display in order to provide uniform viewing. However, it will not be considered here since we shall assume normal incidence light only. In the present geometry, the front polarizer is at an angle $\alpha$ to the input director of the LC cell, which is defined as the $x$-axis. The angle $\alpha$ is positive if it is clockwise from the input director. Likewise, the twist angle $\phi$ is defined as positive if it is a right-handed twist. Basically, this geometry is the same as in ref. 9. If a sheet polarizer is used in the display, which is always the case for direct-view applications, the polarizer is in a $//-//$ arrangement. This is in contrast to the use a polarizing beam splitter (PBS) where the input and output beams are perpendicularly polarized. In that case we would have a parallel–perpendicular ($//-\perp$) polarizer situation, which is suitable for projection display applications. In this paper, we shall deal with direct view multiplexable displays only. For projection displays, an active-matrix is more appropriate, since it eliminates the need for multiplexing and therefore the need for large twist angles. Hence, in the rest of

*[1]Permanent address: Department of Optical Engineering, Zhejiang University, Hangzhou, China.
*[2]Author to whom correspondence should be addressed.
E-mail: eekwok@usthk.ust.hk.

this paper, we shall assume the //−// geometry and direct-view applications.

As discussed in previous papers, the Jones matrix approach is used to obtain the parameter space for the LCD at $V = 0$. The Jones matrix formulation has been described adequately in our previous papers[7–9] and will not be repeated here. It suffices to say that it is an excellent approach to generate the *static* parameter space for any type of nematic LC display, transmittive or reflective. This static parameter space depends on three variables, $\alpha$, $\phi$ and $d\Delta n$. Any pair of these variables can be used to generate a contour map of either the reflectance or the transmittance for visualization of the operation of the LCD.

Figure 1 shows the $\phi - d\Delta n$ parameter space of the RSTN for $\alpha = 0°$. It shows the constant reflectance contour lines in steps of 10%. The pretilt angle of the liquid crystal is assumed to be zero. A wavelength of 550 nm is assumed for the input light. Figure 1 shows clearly a series of minima in reflectance, as indicated by the wells of zero reflectance in the parameter space. They are called the TN-ECB (electrically controlled birefringent) modes, first introduced by Sonehara and Okumura,[10,11] and refined by others subsequently.[7,12,13] For $\alpha = 0$, we showed previously that the TN-ECB minima were given by[7]

$$\phi = \pm(2N-1)\frac{\pi}{2\sqrt{2}} \tag{1}$$

and

$$d\Delta n = \pm(2N-1)\frac{\lambda}{2\sqrt{2}} \quad \text{for} \quad N = 1, 2, 3, \cdots \tag{2}$$

We shall call the first minimum at $\pm 63.6°$ the TN-ECB $\pm$ 1 mode, the minimum at $\pm 190.8°$ the TN-ECB $\pm$ 2 mode, and so on. In ref. 9, we showed how the TN-ECB modes moved around in the parameter space as $\alpha$ was varied. Basically, the TN-ECB modes move towards the center $\phi = 0$ line, with the + and − modes interleaving each other. At $\alpha = 45°$, the parameter space becomes symmetrical with the TN-ECB wells along the $\phi = 0$ line, and are exactly the normal ECB modes. Figure 2 shows the parameter space for the case of $\alpha = 60°$ or $\alpha = -30°$. The asymmetry and the interleaving TN-ECB modes can clearly be seen.

The parameter spaces in Figs. 1 and 2 are generated for a fixed wavelength of 550 nm. In the case of RSTN optimization, since both the select and nonselect states have a strong wavelength dependence, it is useful to plot the reflected *luminance* with white light input. In plotting the luminance, we take the photopic response of the human eye into consideration. Figure 3 shows such a luminance $\phi - d\Delta n$ parameter space for $\alpha = 60°$. It is normalized to give unity luminance along the $x$-axis. The contour lines show decreasing luminance in steps of 0.1. In calculating Fig. 3, we have ignored the wavelength dependence of the liquid crystal properties since we have not specified any one type of liquid crystal. In particular, the dispersion of the refractive indices has not be taken into account. Thus, the result should be considered to be qualitative. In general, the plot in Fig. 3 should be calculated for a specific liquid crystal where the dispersion properties are known. Nevertheless, one can make some important observations using Fig. 3. Comparing it with Fig. 2, the most striking feature is that only the first 2 TN-ECB minima show zero luminance or reflectance. The higher order TN-ECB "minima" no longer have zero reflectance, because even though $R = 0\%$ at one wavelength, it has a large nonzero $R$ at other wavelengths. Figure 4 shows the reflectance of the TN-ECB-2 and TN-ECB-3 modes as a function of wavelength. It clearly illustrates the dispersive nature of these higher order

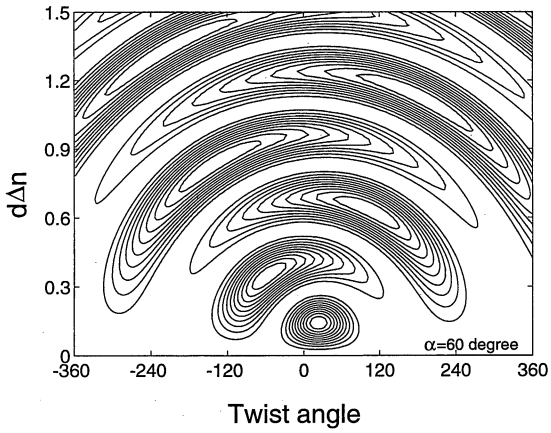


Fig. 2. $\phi - d\Delta n$ parameter space at a polarizer angle $\alpha$ of 60°.

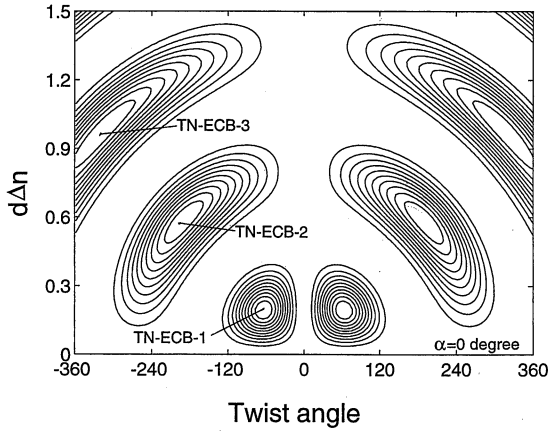


Fig. 1. $\phi - d\Delta n$ parameter space at a polarizer angle $\alpha$ of 0°. The contour lines are lines of constant reflectance in steps of 0.1. Reflectance is equal to 1.0 along the $x$-axis, and zero at the center of the wells.

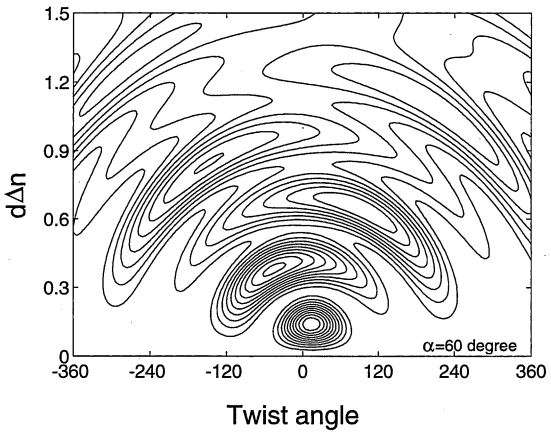


Fig. 3. $\phi - d\Delta n$ parameter space at a polarizer angle $\alpha$ of 60°. White light input is assumed. The reflectance contours are calculated using the photopic response of the human eye.

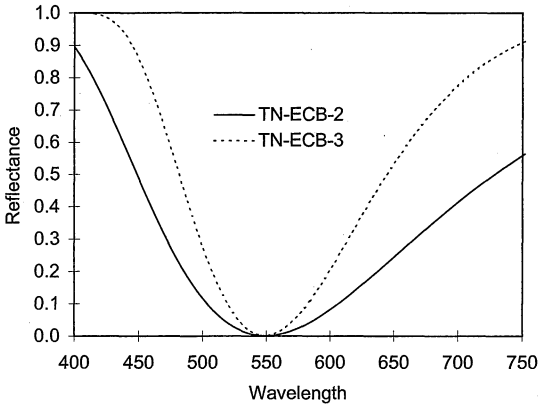


Fig. 4. Calculated reflectance spectra for the second and third TN-ECB modes. The LCD parameters correspond to the wells in Fig. 1.

modes. Therefore Fig. 3 shows that only the lowest TN-ECB modes can achieve a dark state. Therefore, the lowest order TN-ECB minimum should always be used in optimizing the RSTN display.

We shall make use of Figs. 1–3 to make some comments on the design and optimization of the RSTN before plunging into details of the dynamical simulation. In this paper, we shall concentrate on twist angles of 190–240° since we are interested in steep reflectance-voltage curves. Similar to the case of reflective TN displays discussed in ref. 9, there are two possibilities for designing the RSTN. In the first possibility, the $V = 0$ state corresponds to one of the TN-ECB minima. In this case, the display is normally black (NB). These are also called the "in-well" modes. The bright state occurs when $V =$ high so that $\Delta n$ becomes zero.

Alternatively, the $V = 0$ state can be outside the TN-ECB minima (the "out-well" modes). The display will be normally white (NW). The dark state occurs only for carefully chosen combinations of $\alpha$, $\phi$ and $d\Delta n$. Moreover, the dark state occurs only for a finite voltage range. For these NW modes, $V =$ high also corresponds to a bright state as $\Delta n$ becomes zero. Hence it can be seen that the NW operation is much more difficult to optimize than the NB operation. The payoff is that the NW modes can be potentially less chromatic and the operating voltages are always lower since the homeotropic $\Delta n = 0$ state is never utilized.

Note that the nomenclature of NB and NW is specific to the situation of direct view displays (//–// polarizers) with no retardation compensation films. If an achromatic quarterwave film is placed inside the display, black and white can be reversed. Similarly, black and white can be reversed if //– $\perp$ polarizers are used. We shall not consider these cases in this paper.

The NB modes include the TN-ECB mode[10,11] the mixed TN (MTN)[14,15] mode, the self-compensated TN (SCTN)[16] modes and the recently published mixed STN (MSTN).[17] It can be seen from Fig. 1 that they are actually variations of each other with a change in the polarizer angle. For example, as shown in Fig. 1, the second or third TN-ECB minimum actually correspond to the MSTN mode.[17] For these "in-well" modes, the display will become bright at high voltages as $\Delta n$ decreases. These "in-well" operations have several disadvantages. (1) They have relatively large chromatic dispersion. Figure 4 shows the large chromatic dispersion of the second and third TN-ECB minimum. (2) Unlike the "out-well" modes to be discussed later, the NB "in-well" modes have a smaller parameter space. There is basically only one variable for their optimization. For example, if $\alpha$ is given, then $\phi$ and $d\Delta n$ are fixed. Hence, it is impossible to optimize these displays satisfactorily. (3) The bright state relies on achieving homeotropic alignment. Hence, relatively high voltages are required for their operation.

The NW modes are much better in achieving a low chromatic dispersion, high contrast display for direct-view applications. They correspond to the region between the TN-ECB wells in the parameter space, particularly that between the second and third TN-ECB modes. In Fig. 1, the region with $\phi$ from 190° to 240° and $d\Delta n$ from 0.6 to 0.9 $\mu$m can be the initial starting point for such optimization. Note that as $\alpha$ varies, this region of $R = 100\%$ will also shift. The idea is, therefore, to find a ($\alpha$, $\phi$, $d\Delta n$) combination that will produce the $R = 0\%$ state as the voltage is increased. Moreover, that $R = 0\%$ point should be more or less wavelength independent. In general, it is impossible to predict the reflectance of the display as $V$ increases simply from the static parameter space diagram. A full-fledged numerical simulation with the director deformation as a function of voltage is needed. However, since the director does not deform until the Freder-iks transition, we can regard the static parameter spaces in Figs. 1–3 as somewhat valid for the nonselect voltage.

## 3. Numerical Results

The procedure for the optimization of the RSTN mode consists of (1) finding a combination of ($\alpha$, $\phi$, $d\Delta n$) that will lead to low-dispersion $R = 100\%$ operation at $V = 0$ and (2) calculating the reflectance–voltage ($RV$) curves for red, green and blue lights for each such combination. The ($\alpha$, $\phi$, $d\Delta n$) combination that will lead to a low $R$ near 0% and that has low dispersion will be the desired optimized RSTN. In order to obtain the $RV$ curves, we followed the standard procedure for LCD modeling. First, the one dimensional Euler-Lagrange equations for the director deformation were solved to give the director angles $\phi(z)$ and $\theta(z)$ for all values of $z$ inside the LC cell for any value of applied voltage.[18] Then the reflectance was calculated by the extended Jones matrix approach of dividing the cell into many layers and treating each layer as a birefringent plate.[19] Fortunately, many such LCD modeling tools are available. We have written our own code that is especially designed for reflective displays.

Table I summarizes the material parameters used in the numerical simulations. These values are typical for STN displays. A pretilt angle of 5°, which is more in line with the experimental situation, is used in calculating the $RV$ curves. The other parameters are also similar to those of real STN materials. In the simulation, we did not vary the $d/p$ ratio to steepen the $RV$ curves. Hence, there is no elastic strain and $d/p = \phi/2\pi$.

The results for NB RSTN will be presented first. As discussed in the previous section, these are the operating modes which correspond exactly to the TN-ECB minima in the parameter space. As shown in Figs. 1 and 2, the only adjustable parameter is $\alpha$ so the optimization is relatively straightforward. Figure 5 shows the $RV$ curve for a 194° twist cell operating at exactly the second TN-ECB minimum. (A similar result was recently reported by Wu *et al.*[17] and is called

Table I. Values of parameters used in the simulation.

| Parameters | Value |
|---|---|
| $K_{11}$ | $12.6 \times 10^{-12}$ N |
| $K_{22}$ | $6.1 \times 10^{-12}$ N |
| $K_{33}$ | $18.65 \times 10^{-12}$ N |
| $\varepsilon_{//}$ | $108.26 \times 10^{-12}$ F/m |
| $\varepsilon_{\perp}$ | $42.05 \times 10^{-12}$ F/m |
| Pretilt angle $\theta_s$ | 5° |

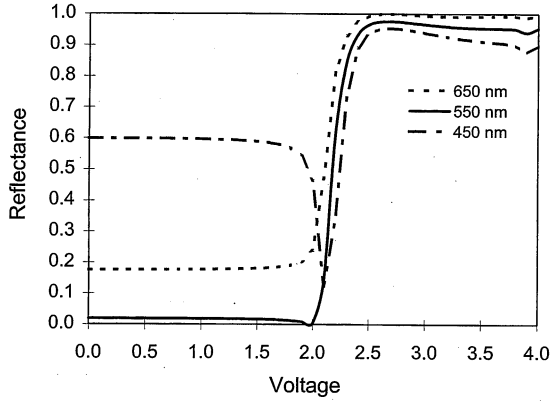


Fig. 5. Calculated $RV$ curves of the NB RSTN (TN-ECB-2 mode). $\phi = 194°$ and $d\Delta n = 0.56\,\mu$m, for $R$ (650 nm), $G$ (550 nm) and $B$ (450 nm).

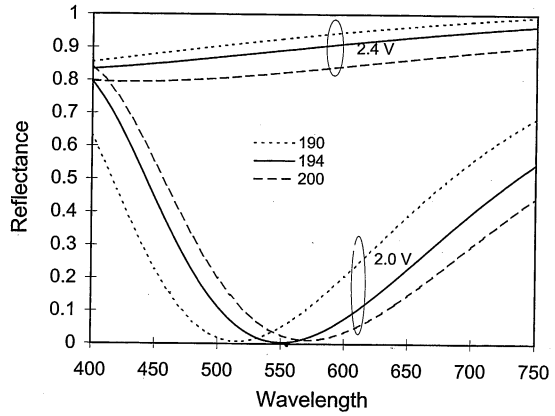


Fig. 6. Calculated reflectance spectra of the NB RSTN in Fig. 5 for several values of $\phi$. The values of $\phi$ are indicated in degrees.

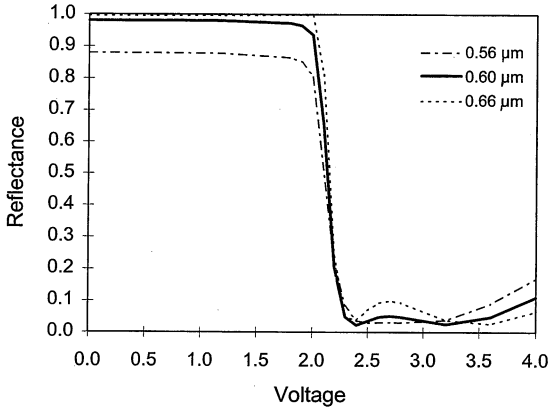


Fig. 7. Calculated $RV$ curve of the NW 194° RSTN using 3 different $d\Delta n$ values. White light input is assumed.

the MSTN mode, but it can be seen here that it is actually a TN-ECB mode.) In Fig. 5, three different wavelengths ($R$, $G$ and $B$) were used in the calculation. It is seen that the $RV$ curve is quite steep, similar to those in conventional STN displays. Saturated maximum reflection is obtained at $V > 2.5$ V. However, there is a large difference between the 3 wavelengths. This dispersion is shown more clearly in Fig. 6 where we plotted the reflectance spectra for both the select (bright at 2.4 V) and nonselect (dark at 2.0 V) states for 3 cells with slightly different twist angles. The $d\Delta n$ values are 0.56 $\mu$m and the polarizer angle is 0°. As predicted, the dark state curves are quite dispersive. They are similar to those in Fig. 4. However, the bright states are very flat. This is understandable because the field-on select state is essentially the homeotropic state. Figures 5 and 6 show that the "in-well" NB operation does not produce a good RSTN.

We next proceed to the examination of the "out-well" NW operation of the RSTN. As seen in Figs. 1 and 2, there is a large area in the parameter space where the display is normally white. There are now two independent parameters, $d\Delta n$ and $\alpha$ for optimizing the RSTN. The procedure for our systematic search for the RSTN modes is as follows. We first generate a series of parameter spaces using $\alpha$ as the parameter.[9] We then search the region between the TN-ECB minima for a low dispersion bright state, near the twist angles of 180° and 240°. The reason for these values for the twist angle is that they are popularly used in common STN displays. For each combination, such as the region near $\phi \sim -200°$ and $d\Delta n \sim 0.5\,\mu$m in Fig. 2, we performed a full dynamical simulation to obtain the $RV$ curves for $R$, $G$ and $B$ colors. A good display mode is defined as one where both the bright and dark states have low chromatic dispersion, and that the dark state has low reflectance. The latter point is very important since the dark state is not guaranteed for the NW RSTN. Only a few combinations of $\alpha$ and $d\Delta n$ can yield a good dark state.

Using this procedure, after some tedious search, we obtained NW RSTN modes with low dispersion near $\phi \sim -194°$, $d\Delta n \sim 0.5\,\mu$m, $\alpha \sim 51°$ and $\phi \sim 240°$, $d\Delta n \sim 0.85\,\mu$m and $\alpha \sim 6°$. Certainly there may be more good RSTN display modes, but we believe that the modes presented here are among the best. Figure 7 shows the $RV$ curve for the first case (194°) using 3 different values of $d\Delta n$. White light is assumed for the input and the photopic response of the eye is taken into account, so that the reflectance refers to the luminance of the display. The $RV$ curves are steep and the reflectance increases again at 3.3 V, i.e., the dark (select) state is only good within a certain voltage range. The reason is quite clear from the parameter space diagram in Fig. 3. At high voltages, the LC cell becomes homeotropic and the reflectance must increase to 100% again necessarily. So near-zero reflectance is achieved only for a finite voltage range. In fact, many ($\alpha$, $\phi$, $d\Delta n$) combinations will not have a decent dark state at all. From Fig. 7, it seems that $d\Delta n$ of 0.6 $\mu$m produces the best luminance and contrast combination. The contrast ratio achievable is about 50 : 1.

Figure 8 shows the entire calculated reflectance spectrum for several voltages. It is seen that it is possible to obtain near-zero reflectance for the RSTN for a single wavelength

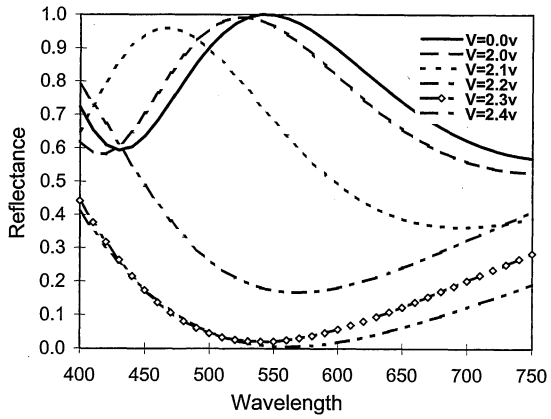


Fig. 8. Calculated reflectance spectra for the NW 194° RSTN at various voltages.

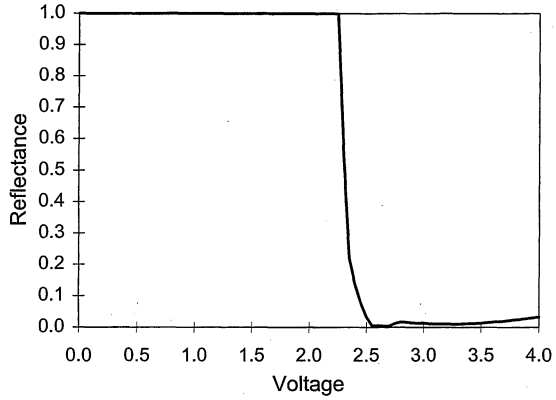


Fig. 9. Calculated $RV$ curve of the 240° RSTN at 550 nm.

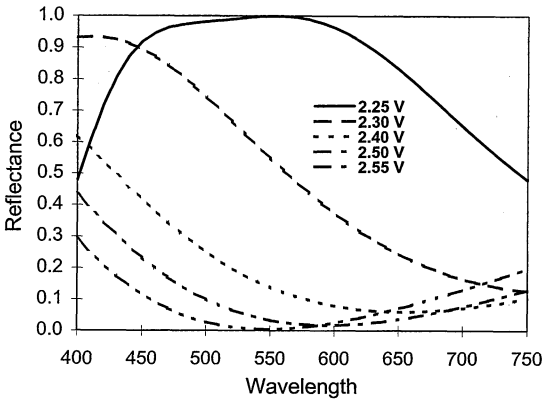


Fig. 10. Calculated reflectance spectra of the 240° RSTN as a function of voltage.

only. Based on Fig. 8, the bright-state (nonselect) voltage should be 2.0 V and the dark-state (select) voltage should be 2.3 V in order to obtain a good contrast and high brightness. The corresponding steepness ratio is 1.15, implying a multiplex number of 50. This number of lines is already good enough for many applications. It can also be seen from Fig. 8 that within the visible wavelength range of 450–700 nm, the reflectance varies by about 30% in the bright state and about 15% in the dark state. Thus, the dispersion properties of the RSTN display are better than those of conventional STN displays.[1–3] The NW RSTN is similar to the "yellow mode", except that the yellow mode has a variation of almost 50% in transmittance for the same visible wavelength range.

Figure 9 shows results of another operation of the RSTN at $\phi$ near 240°. In that figure, the reflectance is plotted as a function of voltage for the case of (6°, 240°, 0.85 $\mu$m). It can be seen that a sharper reflectance drop than the 194° case is obtained, which is expected because of the higher twist angle. The most interesting observation from a practical point of view is that, similar to Fig. 7, the near-zero reflectance region is very wide. The reflectance does not increase again until $V > 3.5$ V. Figure 10 shows the reflectance spectra of this display as a function of applied voltage. This diagram is similar to Fig. 8 except that both the select and nonselect states are slightly less dispersive. Within the visible range, the bright state reflectance varies by 20% while the dark state one varies by 10%. This is again excellent as compared to ordinary STN, and even better than the case of 194° twist. The reflectance steepness is about 1.1 which implies a mux ratio of near 100. It should be mentioned that the steepness ratio, and hence the mux number, of both the 194° and 240° RSTN introduced above can be increased by varying the $d/p$ ratio of the LC cell, as in ordinary STN displays.[4]

## 4. Experimental Results

Many cells were fabricated using the design parameters discussed above. A Merck MLC-5300 and MLC-5400 multibottle system was used to adjust the $d\Delta n$ value of the LC cell to as close to the designed values as possible. An industrial quality LCD fabrication facility in a class 1000 clean room was used to prepare the sample cells.[20] A precise rubbing machine was used to control the twist angle of the cell to within 1° accuracy. The pretilt angle of the liquid crystal was controlled to be about 5°. The electrooptic properties were measured using an automatic data acquisition system and a programmable HP function generator. Both laser and white light sources were used in the measurements. The spectral properties were measured using a Photoscan PR501.

Figures 11 and 12 show the results for the NB "in-well" mode. The parameters are basically the same as those at the TN-ECB second minimum discussed by Sonehara *et al.*[10] The LC cell has a twist of 194° and a $d\Delta n$ value of 0.6 $\mu$m. The polarizer angle is near 5°, which makes it slightly non-TN-ECB. Figure 11 shows the reflectance of the RSTN as a function of the applied voltage at a wavelength of 550 nm. It is in reasonably good agreement with Fig. 5. The onset of reflectance change occurs at 1.5 V. The continued rise in reflectance beyond 2.2 V indicates that homeotropic alignment is not yet complete. This display can operate between 1.7 V (nonselect) and 2 V (select), implying a steepness ratio of 1.17. The $d/p$ ratio of the sample is consistent with the natural twist so that there is no elastic strain on the LC. Figure 12 shows the complete reflectance spectra at 1.5 V and 2.0 V. They are also in general agreement with the calculation in Fig. 6. The select state has a flat reflectance spectrum due to the near-homeotropic alignment. The nonselect dark state however, has a large wavelength dispersion. The experimental results show that this NB operation is not an attractive mode of operation for the RSTN because of the poor contrast ratio with white light input.

Results for the NW 194° RSTN are shown in Figs. 13 and 14. The same LC cell used in Figs. 11 and 12 was employed

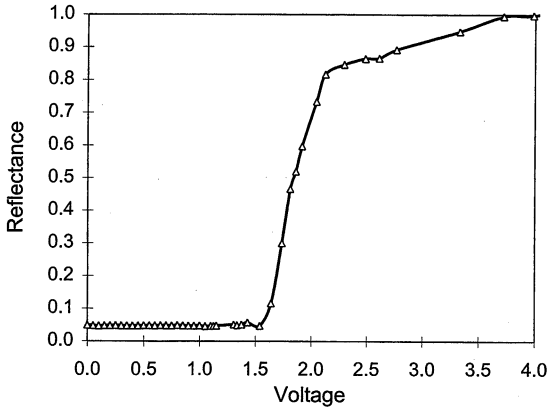


Fig. 11. Experimental reflectance-voltage curve for the NB RSTN.

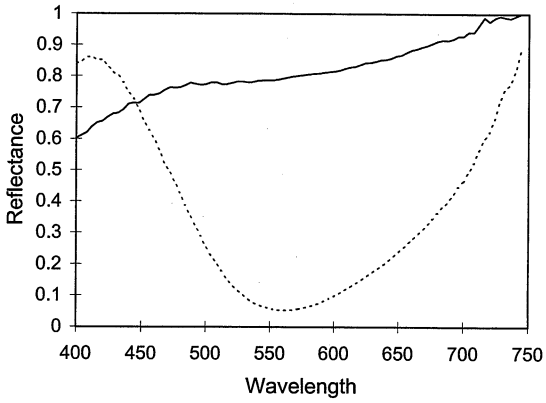


Fig. 12. Experimental reflectance spectra for the NB RSTN.

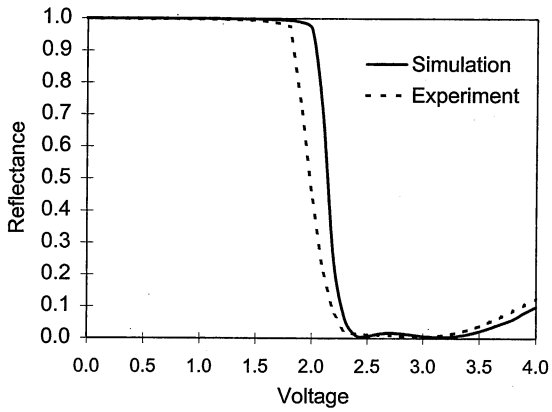


Fig. 13. Experimental reflectance-voltage curve for the NW 194° RSTN (dotted line). The solid line is the calculated result.

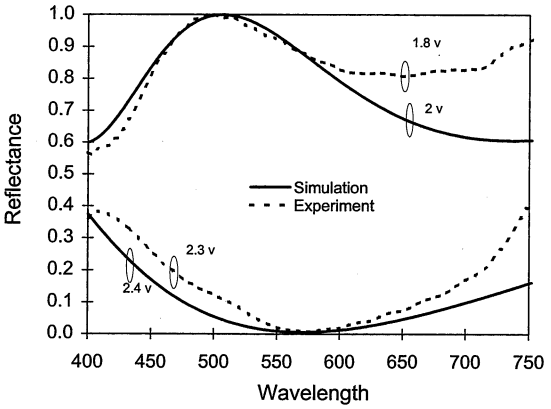


Fig. 14. Experimental reflectance spectra for the NW 194° RSTN (dotted line). Solid line indicates the theoretical values.

and the polarizer angle was about 51°. Figure 13 shows the RSTN reflectance-voltage curve measured with a HeNe laser at 632 nm. The dotted line indicates the experimental result and the solid line the theoretical prediction. In this case, the agreement between experiment and theory is better than in the NB case. In fact, the agreement is quite good considering that no adjustable parameters were used in the simulation to fit the data. It should be noted that since a single wavelength is used, a perfect zero reflectance can be obtained.

Figure 14 shows the entire reflectance spectrum for the NW case. Measurement results for both the dark state and the bright state are depicted. Again, the solid line is the theoretical curve while the dotted line shows the experimental data. The agreement is also quite good in the central wavelength region. The disagreement between the experimental and theoretical curves in the long wavelength region is due to the light detector which does not have good sensitivity in this wavelength region and tends to be rather noisy. Nevertheless, the general trends agree with those in the predictions. The dark state for the NW operation in Fig. 14 is much darker than the NB dark state in Fig. 12. If one integrates the reflectance spectrum over the visible spectrum weighted by the standard photopic curve, an overall luminance contrast ratio of 20 : 1 is found to be achieved with the RSTN. This is good enough for many commercial applications.

Finally, the $RV$ curve and the reflectance spectrum for the 240° RSTN are shown in Figs. 15 and 16, respectively. In the RV curve in Fig. 15, white light was used for illumination. It is seen that the steepness is similar to that of the theoretical curve in Fig. 9. However, the dark state does not reach zero reflectance since Fig. 9 was calculated at 550 nm while the experimental curve was obtained with white light. Figure 15 indicates that the white light contrast for this RSTN is about 12 : 1. The steepness ratio using the select and nonselect voltages shown is about 1.104. The reflectance spectrum in Fig. 16 was taken at the select voltage and nonselect voltages shown. The dispersion is higher than the theoretically predicted one in Fig. 10. The reason for this may be the dispersion of the liquid crystal and the detection system. It is, however, still better than that of an ordinary STN without film compensation.

## 5. Conclusions

In summary, we have demonstrated that a reflective STN display can be made without a rear polarizer. The general range of the twist angle is 190–240°. By searching the parameter space of the twist angle, the polarizer angle and the birefringence of the liquid crystal cell, we were able to identify many operating points for a reflective RSTN with high reflectivity, excellent contrast and good color dispersion. Full dynamical simulation was performed to obtain the voltage-dependent reflectance of this display, from which the select and nonselect voltages could be obtained.

Experimental cells were fabricated. The measured reflectances were in good agreement with the theoretical predic-

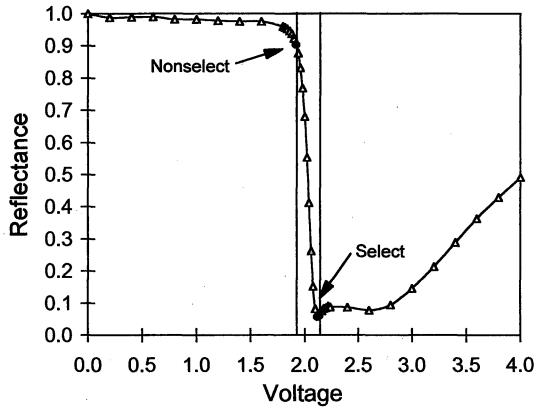


Fig. 15. Experimental reflectance-voltage curve for the NW 240° RSTN. White light is used as the input. The select and nonselect voltages are shown.

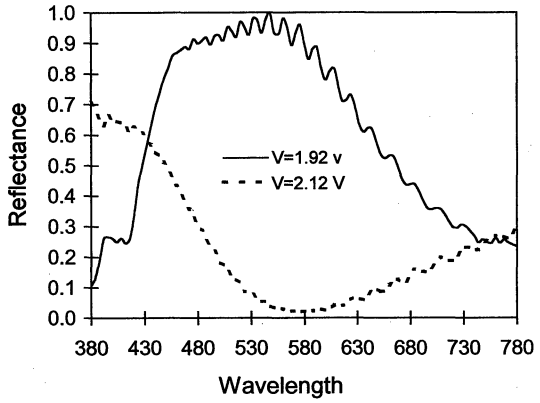


Fig. 16. Experimental reflectance spectra for the NW 240° RSTN. Operating voltages are indicated.

tions. Both the reflectance-voltage curve and the reflectance spectra were in excellent agreement with theory. The results show that the parameter space approach is powerful for searching for new LCD display modes. The optimized RSTN mode discussed here should also find applications in low-power high-brightness display systems. It should be emphasized that the RSTNs introduced here are compatible with ordinary STN displays in terms of manufacturing. The cell gap, twist angles and LC materials are all very similar. Therefore, it is very easy to adapt the manufacturing process of the ordinary STN to this new RSTN. The only added optical element is the light diffuser film.[5,15]

Recently, a noncompensated STN (XSTN)[21] display was proposed by Wang *et al.* This XSTN has a twist angle larger than 90°. No further details were given and only simulation results were shown. Judging from the published figures, the XSTN is not as good as the RSTN discussed here in terms of the steepness of the $RV$ curve and the contrast of the display. We expect the RSTN discussed in this paper to be a good alternative to conventional STNs in many applications.

This research was supported by the Hong Kong Industry Department, Industry Technology Development Council.

1) J. Scheffer and J. Nehring: J. Appl. Phys. **58** (1985) 3022.
2) M. Schadt and F. Leenhouts: Appl. Phys. Lett. **50** (1987) 236.
3) K. Kawasaki, K. Yamada, R. Watanabe and K. Mizunoya: SID Symp. Dig. **18** (1987) 391.
4) L. M. Blinov and V. G. Chigrinov: *Electrooptic Effects in Liquid Crystal Materials* (Springer-Verlag, New York, 1994).
5) T. Uchida: SID Symp. Dig. **27** (1996) 31.
6) W. D. St. John, Z. L. Lu and J. W. Doane: J. Appl. Phys. **78** (1995) 5253.
7) H. S. Kwok: J. Appl. Phys. **80** (1996) 3687.
8) S. T. Tang, F. H. Yu, J. Chen, H. C Huang, M. Wong and H. S. Kwok: J. Appl. Phys. **81** (1997) 5924.
9) F. H. Yu, J. Chen, S. T. Tang and H. S. Kwok: submitted to J. Appl. Phys. 1997.
10) T. Sonehara and O. Okumura: Japan Display, Proc. 9th Int. Display Research Conf. (Society for Information Displays, 1989) Vol. 9, p. 192.
11) T. Sonehara: Jpn. J. Appl. Phys. **29** (1990) L1231.
12) V. Konovalov, A. Muravksi, S. Yakovenko, A. Smirnov and A. Usenok: SID Symp. Dig. **27** (1996) 615.
13) K. Lu and B. E. A. Saleh: SID Appl. Dig. **27** (1996) 63.
14) S. T. Wu and C. S. Wu: Appl. Phys. Lett. **68** (1996) 1455.
15) C. K Wei, C. L. Kuo, C. W. Hao, C. L Chen, D. L. Ting, Y. C. Chen, C. W. Wang, P. Y. Tang and C. M. Ting: Proc. Fourth Asian Symp. Information Display, eds. H. S. Kwok and M. Wong, Hong Kong, 1997, p. 25.
16) K. H. Yang: Euro-Display, Proc. 16th Int. Display Research Conf. (Society for Information Display, 1996) p. 449.
17) S. T. Wu, C. S. Wu and C. L. Kuo: SID Appl. Dig. **28** (1996) 643.
18) M. Schadt and W. Helfrich: Appl. Phys. Lett. **18** (1971) 127.
19) A. Lien: J. Appl. Phys. **67** (1990) 2853.
20) See *http://www.ee.ust.hk/~cdr/* for details of this LCD prototyping line.
21) X. J. Wang, S. S. Chen and X. J. Zhang: Proc. Fourth Asian Symp. Information Display, eds. H. S. Kwok and M. Wong, Hong Kong, 1997, p. 15.